Check for updates

www.ietdl.org

Published in IET Renewable Power Generation
Received on 6th October 2013
Revised on 3rd February 2014
Accepted on 14th February 2014
doi: 10.1049/iet-rpg.2013.0318

Special Issue: European Wind Energy Association 2013

ISSN 1752-1416

Comparison of methods for wind turbine condition monitoring with SCADA data

Michael Wilkinson, Brian Darnell, Thomas van Delft, Keir Harman

DNV GL-Energy, Renewables Advisory, St Vincent's Works, Silverthorne Lane, Bristol BS2 0QD, UK
E-mail: Michael.Wilkinson@dnvgl.com

Abstract: Wind turbine operational costs can be reduced by monitoring the condition of major components in the drivetrain. SCADA-based condition monitoring is attractive because the data are already collected, resulting in rapid deployment and modest set-up cost. Three SCADA-based monitoring methods were reviewed: signal trending; self-organising maps and physical model. The physical model was identified as being the most reliable at predicting impending component failures. A validation study on this method using five operational wind farms showed that it is possible to achieve a high detection rate and good detection accuracy. An advance detection period of between 1 month and 2 years was achieved by the method. The study has also highlighted limitations and areas for further development.

1 Introduction

Wind turbine reliability remains an important focus for wind turbine owners, operators and manufacturers. There is an economic case in favour of condition monitoring for rotating machines in general [1] and also specifically for wind turbines [2]. The effect of low reliability on wind turbine and wind farm availability is particularly acute in the offshore environment, where access restrictions mean that a failure can lead to prolonged downtime.

Fig. 1 presents the distribution of annual average availability from a large sample of operating wind farms [3]. From Fig. 1, it can be seen that there remains a significant gap between the highest (50% exceed 97.5%) and lowest availabilities (10% fall below 92.5%). This indicates there is a potential opportunity to make improvements in wind farm availability. A key factor for good wind farm availability is high turbine reliability; reliability can be improved and downtime reduced through the use of condition monitoring [4]. The use of SCADA data for condition monitoring has a number of advantages; in particular, the data are already collected, requiring no additional hardware.

Different approaches are available to utilise SCADA data to predict the health of operational wind turbines, for example: signal trending, artificial neural networks (ANN) and physical models. This paper describes the results of an investigation into these approaches: examples of application to real datasets are given and the relative merits are compared. The method that was found to be most effective was then subjected to a large validation study, which tested the effectiveness of the techniques in detecting a range of different component failures on 472 wind farm years of SCADA data from multiple turbine manufacturers.

2 Review of methods

An investigation has been undertaken into three different approaches available for condition monitoring with SCADA data.

2.1 Signal trending

The approach of signal trending [5] generally involves comparing one turbine against another or one period of time against another. For example, when the gearbox temperature on one turbine rises compared with a neighbour, this may indicate an impending failure. This approach can be further refined through the application of appropriate filtering such as only comparing when the turbines are operational or normalising a component temperature with an external ambient temperature.

An example of this technique is provided in Fig. 2, which shows a time series of normalised temperature of a drivetrain component in a test turbine compared to four control turbines. The time series was derived from 10 minute SCADA data by normalising the temperature of the component to the wind farm average component temperature, calculated for each 10 minute record. The average component temperature in the wind farm is assigned a value of 100%. Periods of missing SCADA data in Fig. 2 are shown by a straight line, although this does not affect the results. The increasing deviation of the test turbine compared with the control turbines corresponds to increasing wear on the drivetrain component, and indicates an elevated risk of failure. In this particular example, the deviation was subsequently found to correspond with damage to the main bearing on this turbine.

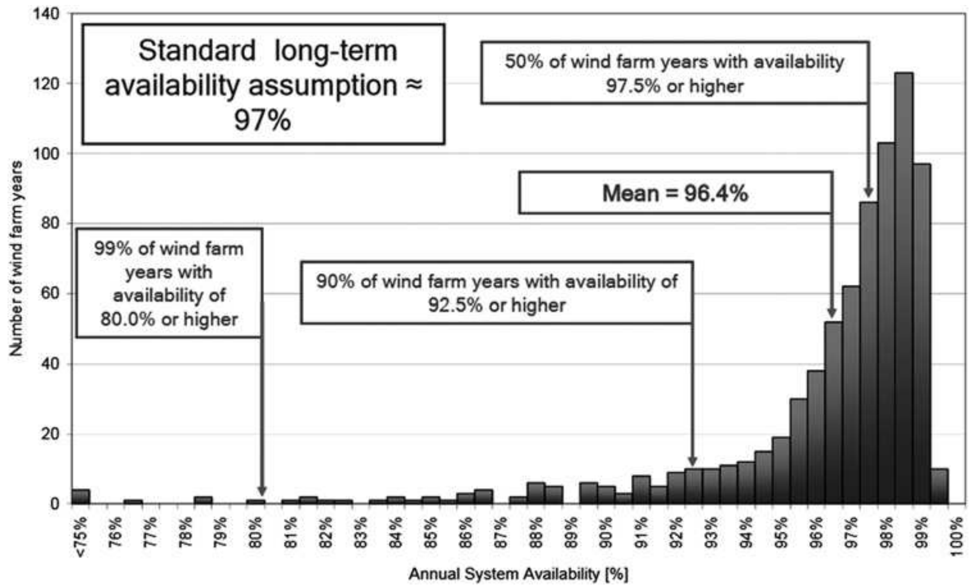

Fig. 1 *Distribution of annual average wind farm availability, reproduced from [3]*

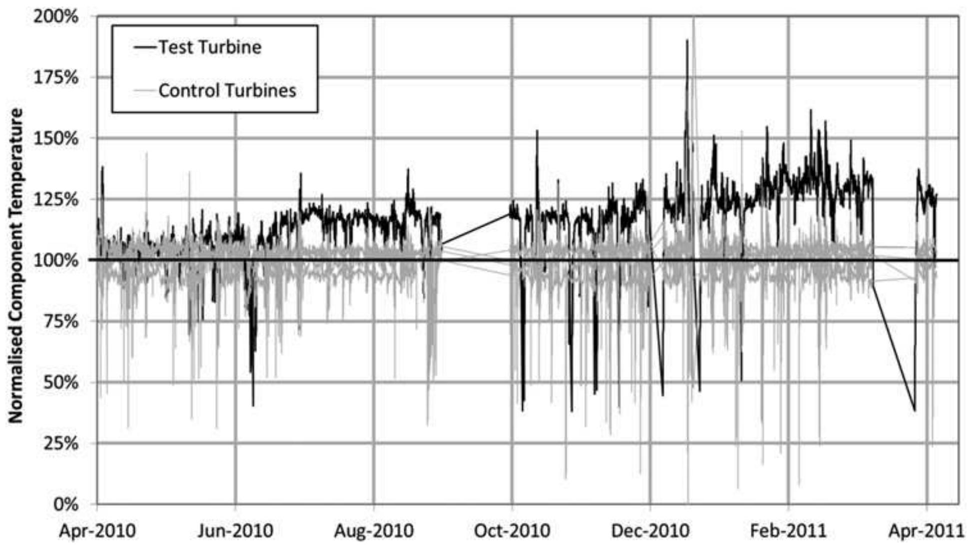

Fig. 2 *Time series of normalised component temperature of a test turbine compared with four control turbines*

2.2 ANN methods

An ANN is a learning algorithm that is used to reveal patterns in data or to model complex relationships between the variables. In terms of wind turbine condition monitoring, ANNs have the potential to identify changes in the relationships between SCADA signals that indicate the development of a failure [6, 7].

Multiple ANN methods have been investigated and the self-organising map (SOM) [8] has been identified as promising in this context. SOMs are used to group similar phenomena in a dataset, with their topographical representations visualising high dimensional data. The application of SOM methods for the purpose of wind turbine condition monitoring has previously been explored, with some success [9], and this technique is investigated further in this study.

2.2.1 Map generation algorithm: The algorithm used to produce a SOM map for condition monitoring analysis is as follows:

1. Choose the most appropriate data signals for the analysis (pre-processing if necessary), selecting a period of data that represents the full range of normal operation.
2. Clean the data of spurious values.
3. Normalise the data.
4. Randomise the map's nodes' weight vectors.
5. Randomly select an input data vector (i.e. data for one timestamp).
6. Traverse every node in the map.
   i. Find the Euclidean distance between the input vector and the node's weight vector.
   ii. Determine the closest node (the 'best matching unit', BMU).
7. Update the nodes in the neighbourhood of the BMU by pulling them closer to the input vector according to

$$\boldsymbol{m}_i(t+1) = \boldsymbol{m}_i(t) + \boldsymbol{\alpha}(t)\boldsymbol{\theta}(t)\big[\boldsymbol{x}(t) - \boldsymbol{m}_i(t)\big]$$

where t is the current iteration, $\boldsymbol{m}_i$ is the node vector, $\boldsymbol{x}$ is the

© The Institution of Engineering and Technology 2014

17521424, 2014, 4, Downloaded from https://ietresearch.onlinelibrary.wiley.com/doi/10.1049/iet-rpg.2013.0318 by CAPES, Wiley Online Library on [07/05/2024]. See the Terms and Conditions (https://onlinelibrary.wiley.com/terms-and-conditions) on Wiley Online Library for rules of use; OA articles are governed by the applicable Creative Commons License

input vector, $\boldsymbol{\alpha}$ is the learning rate and $\boldsymbol{\theta}$ is the neighbourhood function, respectively.

8. Increment t and repeat from step 5 until every input data vector has been applied to the map.
9. Repeat steps 5–8 a number of times to refine the map.

2.2.2 Example – turbine production curtailment: To illustrate how a SOM groups together similar phenomena, Fig. 3 shows a SOM generated from wind speed and power signals during a period in which some power de-rating occurred. The unified distance matrix (U-matrix) map shows where similarities exist in the relationship between inputs. The light colours on the U-matrix show how the data branches into two forks. The corresponding map nodes on the wind speed layer and power layer show that one fork consists of high wind speed and high power and the other consists of high wind speed and low power, the latter being de-rating.

2.2.3 Comparing datasets: SOMs also allow one dataset to be measured against another, thus allowing a dataset that potentially contains a developing failure, to be compared with a benchmark dataset of normal operation. This is achieved by the following method:

1. Generate a SOM in the method described above using a benchmark dataset.

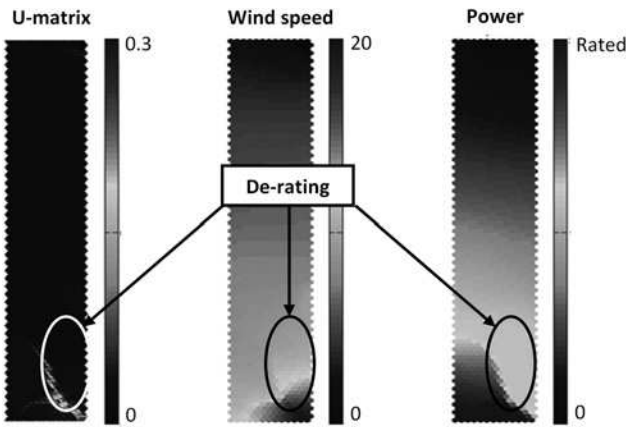

Fig. 3 *Application of SOM methods to identify a power performance effect*

2. With the test dataset, take the same signals and apply the same pre-processing and normalisation factors that were used in generating the map.
3. Select the first data point in the test dataset.
4. Traverse every node in the map.
   i. Find the Euclidean distance between the input vector and the node's weight vector.
   ii. Determine the BMU in the map.
   iii. Calculate the distance between the input vector and the BMU's weight vector – this is known as the 'quantisation error'.
5. Select the next data point in the new dataset and repeat step 4 until each one has an associated quantisation error.

Applying this method to wind turbine SCADA data produces a time series of quantisation errors which describe the deviation of the test dataset from the benchmark dataset. Fig. 4 shows increasing quantisation errors in the months prior to gearbox failures.

2.3 Physical models

A description of the physical model general approach is given in [10] and a report on using the relationship between SCADA signals for failure detection in gearboxes is presented in [11].

The energy balance for a generic component in the wind turbine drivetrain is presented in Fig. 5. It shows that the component temperature, T, depends on the mechanical power delivered, the component rotational speed, the cooling system duty (if applicable) and the surrounding temperature. Therefore a model that predicts the component temperature should include these properties.

The configuration of the wind turbine drive trains were used to inform the choice of input variables used in the model. In some cases, it was necessary to know the setup of the cooling system and signals such as oil/cooling water temperature, pump/fan status etc.

To predict the component temperature, an algorithm was developed using a number of test datasets. For i input signals, the correlation was of the form

$$T'_{\mathrm{Est}} = \frac{R_1^2(m_1x_1 + c_1) + R_2^2(m_2x_2 + c_2) + \cdots + R_i^2(m_ix_i + c_i)}{R_1^2 + R_2^2 + \cdots + R_i^2}$$

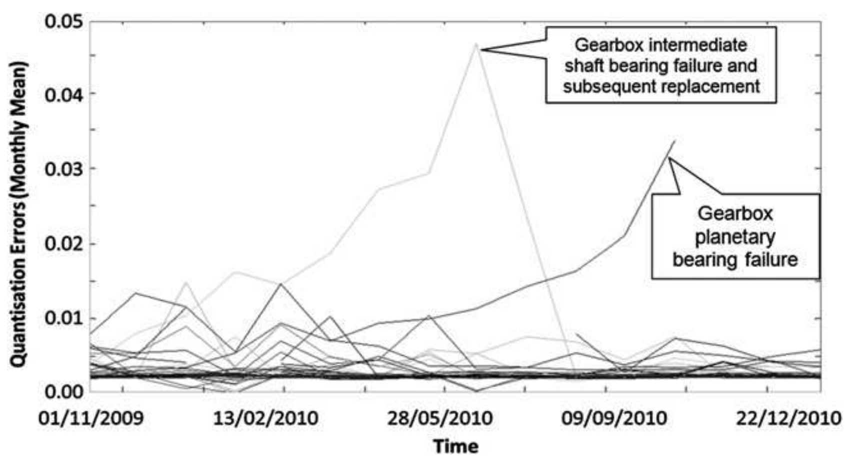

Fig. 4 *Time series of quantisation errors of gearbox temperatures*

© The Institution of Engineering and Technology 2014

doi: 10.1049/iet-rpg.2013.0318

17521424, 2014, 4, Downloaded from https://ietresearch.onlinelibrary.wiley.com/doi/10.1049/iet-rpg.2013.0318 by CAPES, Wiley Online Library on [07/05/2024]. See the Terms and Conditions (https://onlinelibrary.wiley.com/terms-and-conditions) on Wiley Online Library for rules of use; OA articles are governed by the applicable Creative Commons License

17521424, 2014, 4, Downloaded from https://ietresearch.onlinelibrary.wiley.com/doi/10.1049/iet-rpg.2013.0318 by CAPES, Wiley Online Library on [07/05/2024]. See the Terms and Conditions (https://onlinelibrary.wiley.com/terms-and-conditions) on Wiley Online Library for rules of use; OA articles are governed by the applicable Creative Commons License

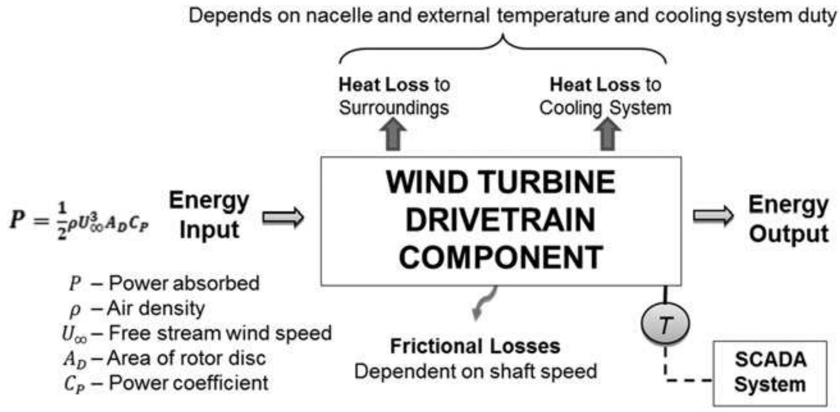

Fig. 5 *Energy balance for a wind turbine drivetrain component*

where R_i^2 is the coefficient of determination for the input signal i, m_i is the gradient of correlation for the input signal i and c_i is the offset of correlation for the input signal i.

Higher order polynomials were applied in some cases (up to ninth order) where they resulted in a higher overall coefficient of determination, in order to improve the model accuracy. The appropriate order depends on the physics of the underlying relationship between the signals. There is a trade-off between the computational overhead and model accuracy, and this is a potential area of future research.

The model parameters were determined over a chosen ‘training period’, which broadly represented ‘normal’ operation. This period was selected by excluding any periods of known or observed deterioration in component health. In some cases, an iterative approach was required to determine a suitable training period.

To identify deterioration in component health, the modelled variable was compared with the actual measured variable. The underlying detection principle relies on deteriorating component health causing the model relationship to change, for example, heat transfer may increase or decrease in rate, or an alternative heat transfer path may be set up. By plotting the rolling average or cumulative model deviation (actual – predicted) over time, it was possible to discern trends that imply deviation from the relationships established during the training period. Often these deviations result from additional frictional heat generated because of accelerated wear of a drivetrain component.

In addition to temperatures, the method has been applied to other low-frequency signals such as coolant pressure, cooling system duty, pitch motor duty cycle etc., depending on the signals available in the turbine SCADA system.

The initial development of the SCADA-based condition monitoring process focused on the continuous variables available from the SCADA system. As an extension of this, it is possible to incorporate digital (binary) data from those turbines which record and store this information in their SCADA data logger. These are status signals indicating one of two states of a component. Examples include: gearbox lubricating pump on/off; generator cooling water pump on/off; generator fan on/off; bypass gearbox filtration unit.

In one of the wind turbines studied, the status signals were combined as bitwise flags into five decimal channels. The channels were available as part of the normal SCADA data output and report a snapshot of the status of the turbine at 10 min intervals. Each of these decimal channels contained either 16 or 32 bitwise flags. Each flag reflects the digital inputs or outputs of the control system. Binary ‘1’ means there is 24 V at the input/output. Binary ‘0’ means the signal is 0 V. Each binary flag was extracted from the decimal signal using a bitwise logical AND operation.

An investigation was undertaken into the available signals and some success has been achieved using the generator fan on/off digital signal. On one particular site, it was found that this fan was switched on or off depending on changes in the operating condition, such as component temperature,

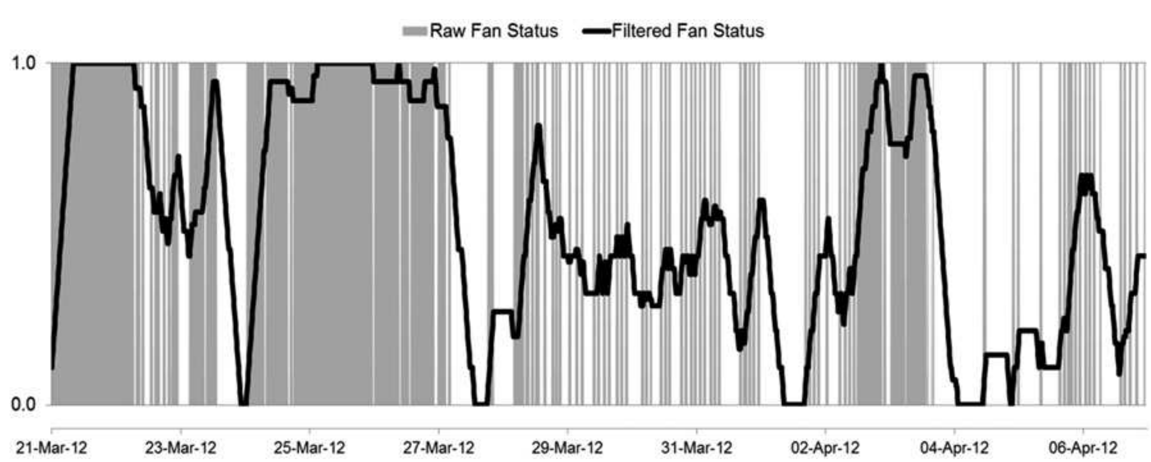

Fig. 6 *Generator fan status: raw (grey) digital signal, and filtered (black) continuous signal*

© The Institution of Engineering and Technology 2014

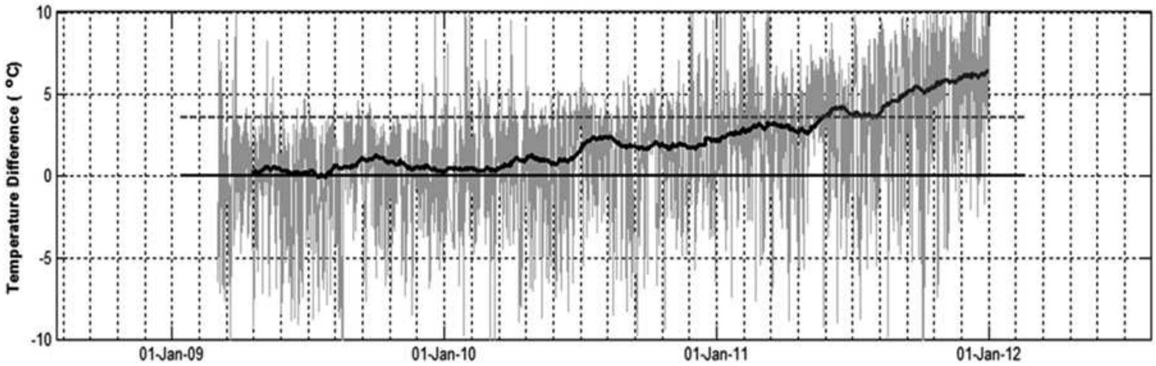

Fig. 7 *Deviation from model for temperature sensor of a main bearing (grey line) overlaid with rolling average (black line)*

Table 1 Scoring of methods

Criteria	Signal trending	SOM	Physical model
Time and effort to initiate a new model for each turbine analysis	3	2	1
Ability to incorporate a wide range of model inputs	1	3	2
Ease of identifying impending component failure	2	1	3
Ability to distinguish component deterioration for operational or environmental fluctuations	1	2	3
Ability to detect impending failures in advance	2	1	3
Total score	9	9	12

power output and ambient temperature. The status of the fan affected the rate of cooling of the generator.

The digital signal was incorporated into the model by transforming it to a continuous variable by applying a low-pass rectangular window filtering function (see Fig. 6). When this continuous variable was included in the generator model, it helped to improve the accuracy because variations in generator temperature because of the cooling effect of the fan could now be accounted for. The new model was able to retrospectively detect a generator issue which had hitherto remained undetected.

As a result of this work, two generator models have been developed. One model is used to monitor the generator bearing health and another is used to monitor the generator stator winding health. The model accuracy at most turbines was sufficient to enable underlying trends to be readily identified, that is, the magnitude of the trend was larger than the noise in the model output. Historical deviations in the models were found to correlate with the previously reported generator failures. A deviation was observed for a generator bearing which had been reported as running with increased acoustic emissions.

It is expected that there will be further opportunities to incorporate digital signals. The extent to which this is beneficial will depend on the specific digital signals that are available from each turbine model.

Fig. 7 shows an example of the output available from the physical model approach, showing a trend in the rolling average of the temperature sensor of the main bearing. The upward trend indicates excessive wear, requiring follow-up action such as inspection of the component.

2.4 Conclusions from the comparison study

All the three approaches studied demonstrated the ability to detect component failures in advance. To select a method for a detailed validation study, each was applied to a single dataset containing several known component failures. The purpose was to understand which model would be most suitable to develop further as a condition monitoring technique. Therefore the models were ranked according to a set of criteria as listed in Table 1. The best performing method for each criterion was assigned a score of 3, and the worst was assigned a score of 1.

The signal trending approach benefits from being simple and readily applied to many datasets. However, the comparison study found that it was not sufficiently accurate or reliable to account for intermittent changes in temperature caused by differing operational modes or external environmental conditions.

The SOM method was observed to be more sensitive to faults than the other approaches and so has some value in the investigation of wind turbine health. The main drawback of the SOM method, as well as other ANN methods, is its inability to identify the nature of abnormal operation. This makes identification of impending failures more difficult.

The physical model approach required the most effort in the initial setup and tuning of the models, and in the definition of suitable training periods. However, once the model had been established, it was found to have

Table 2 Results of the validation study carried out on the physical model technique

Site	Location	Operational dataset years	Predicted failures	Actual failures	True detections	False detections	Score true/false
A	Italy	4.8	7	8	7	0	88%/0%
B	Ireland	6.0	7	8	6	1	75%/13%
C	Ireland	6.5	1	4	1	0	25%/0%
D	UK	7.0	5	6	5	0	83%/0%
E	UK	2.5	7	10	5	2	50%/20%

© The Institution of Engineering and Technology 2014
doi: 10.1049/iet-rpg.2013.0318

17521424, 2014, 4, Downloaded from https://ietresearch.onlinelibrary.wiley.com/doi/10.1049/iet-rpg.2013.0318 by CAPES, Wiley Online Library on [07/05/2024]. See the Terms and Conditions (https://onlinelibrary.wiley.com/terms-and-conditions) on Wiley Online Library for rules of use; OA articles are governed by the applicable Creative Commons License

Modelled Temperature	Rotor Side High Speed Bearing
Model Inputs	Generator Speed Power Nacelle Temperature
Failed Component	Gearbox
Advance notice	9 months

Modelled Temperature	Gen Side Intermediate Speed Bearing
Model Inputs	Generator Speed Power Nacelle Temperature
Failed Component	Gearbox
Advance notice	7 months

Modelled Temperature	High Speed Mid Gear Bearing
Model Inputs	Rotor Speed Power Nacelle Temperature
Failed Component	Gearbox
Advance notice	3 months

Modelled Temperature	High Speed Gen-Side Gear Bearing
Model Inputs	Rotor Speed Power Nacelle Temperature
Failed Component	Gearbox
Advance notice	8 months

Modelled Temperature	Main Bearing
Model Inputs	Rotor Speed Power Nacelle Temperature
Failed Component	Main Bearing
Advance notice	7 months

Modelled Temperature	Gearbox
Model Inputs	Power Nacelle Temperature
Failed Component	Gearbox
Advance notice	2.5 months

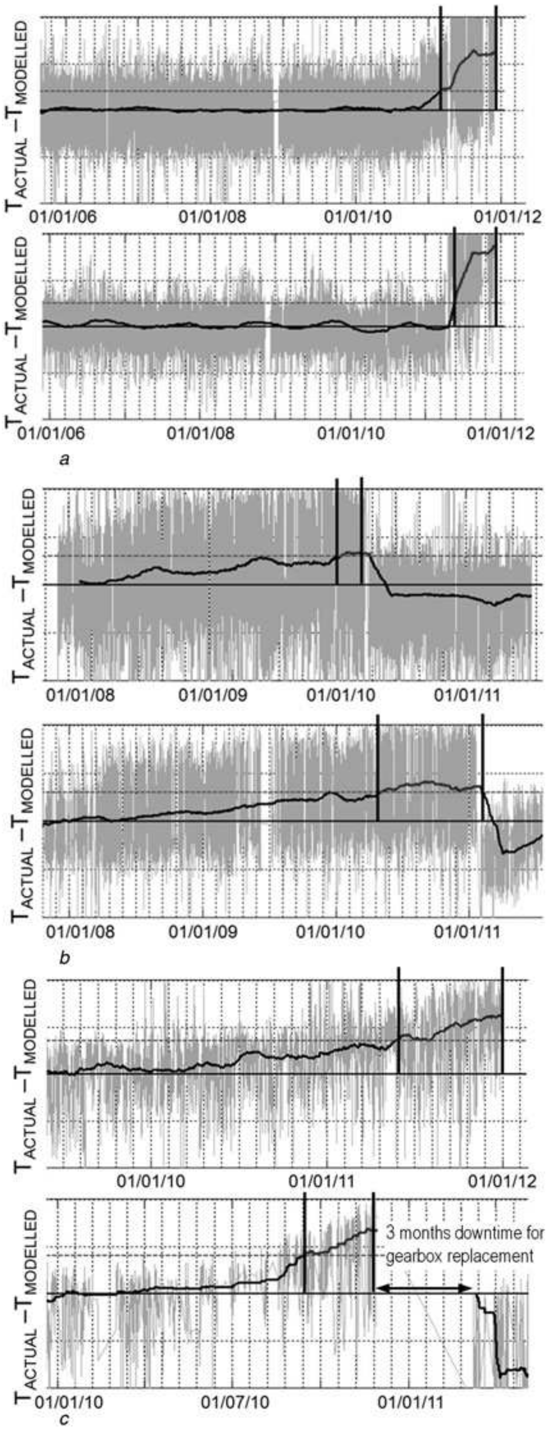

Fig. 8 *Example results from the validation study carried out on the physical model condition monitoring technique*

a Different signals on the same turbine
b Two different turbines at the same site
c Two different turbines at different sites

the most success at identifying abnormal conditions. It produced results which were concise and easy to interpret.

In summary, the physical model method was judged to be the most successful of the approaches. Therefore this technique was investigated further in order to measure its success when applied to a range of datasets. The signal trending and ANN methods did not score as highly and therefore were not investigated any further within the scope of this study. However, this does not rule them out as valuable techniques and further studies could be undertaken to validate these methods.

3 Validation study

A large validation study was performed to determine the effectiveness of the physical model method in detecting impending failures.

© The Institution of Engineering and Technology 2014

17521424, 2014, 4, Downloaded from https://ietresearch.onlinelibrary.wiley.com/doi/10.1049/iet-rpg.2013.0318 by CAPES, Wiley Online Library on [07/05/2024]. See the Terms and Conditions (https://onlinelibrary.wiley.com/terms-and-conditions) on Wiley Online Library for rules of use; OA articles are governed by the applicable Creative Commons License

3.1 Description of the study

Blind tests were conducted on a number of wind farms: a total of 472 turbine-years of data were considered including turbines from multiple manufacturers, ranging between 2.5 and 7 operational years, with different component signals available from each turbine type. The sites are listed in Table 2. The physical model was used to retrospectively determine the approximate failure date and also the approximate date at which the deviation from the model indicates unusual component behaviour.

The actual failure details were then determined by studying additional data such as operation and maintenance reports.

Events where the suspected and actual failures agree were deemed 'true detections'. Where a failure was suspected, but could not be confirmed in the operation or maintenance reports, it was deemed a 'false detection'.

3.2 Example detections

Fig. 8 shows the examples of output from the physical model, where a component failure has been retrospectively detected. The figure provides information on the component that was monitored, the inputs to the model and how far in advance the failure was detected.

For each time series in Fig. 8, the first vertical line corresponds with the point where the model deviation exceeds a chosen threshold value, and the second vertical line indicates where the component was reported to have actually failed.

3.3 Results

The overall results of the study are summarised in Table 2. A high detection rate and a good true:false ratio was achieved for sites A, B and D. These sites demonstrate that the method has good potential for advance detection of component failures.

The detection rate was poor at C and moderate at E. This indicates that there may be some types of component failures which do not lend themselves to reliable advanced detection using this method. For example, component deterioration that does not affect any of the measured

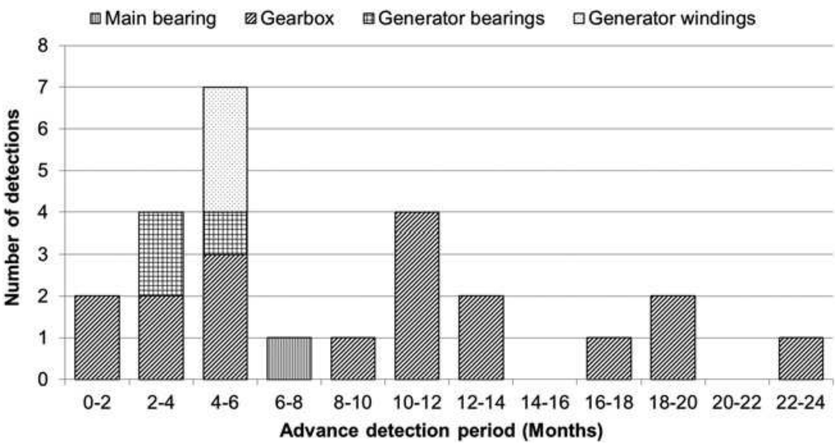

Fig. 9 *Advance detection period of failures identified in the validation study*

Table 3 Method for calculation of confidence factor

Subfactor	Calculation	Score	Maximum
Accuracy of model	use R^2 or adjusted R^2 if available		1.0
Accuracy predicting historical failures across site	%; True detections $= \dfrac{\text{No. of failures correctly detected}}{\text{Total failures}^*}$		1.0
Inaccuracy predicting historical failures across site	%; False detections $= \dfrac{\text{No. of incorrect detections}}{\text{Total failures}^*}$		0.0 (minimum = –5.0)
Duration of training period	no. of months/60		1.0 (no additional credit for training period longer than 60 months)
Duration of deviation	no. of months/12		1.0 (no additional credit for deviation longer than 12 months)
Magnitude of deviation	$\dfrac{\lvert\text{Average deviation}\rvert}{3 \times \text{threshold}}$		1.0 (no additional credit for deviation more than 3× threshold)
Total score			5.0
CF	total score/5.0 × 100%		100%

*Total failures = number of reported failures that would 'normally' be detected using SCM. This might exclude failures such as cracks in generator casing, sudden gear tooth failure etc.

© The Institution of Engineering and Technology 2014
doi: 10.1049/iet-rpg.2013.0318

17521424, 2014, 4, Downloaded from https://ietresearch.onlinelibrary.wiley.com/doi/10.1049/iet-rpg.2013.0318 by CAPES, Wiley Online Library on [07/05/2024]. See the Terms and Conditions (https://onlinelibrary.wiley.com/terms-and-conditions) on Wiley Online Library for rules of use; OA articles are governed by the applicable Creative Commons License

SCADA signals prior to their failure. This is a source of further investigation as it may be possible to improve detection by including alternative signals from the turbine into the model.

A poor true:false ratio was achieved at site E. This site was also found to have poorer quality correlations. It was concluded that this is due to two reasons: (i) the duration of operational data available for the validations was relatively short at 2.5 years; (ii) the timing of component failures was uncertain, resulting in challenges for the definition of suitable training periods

3.4 Advance detection

The validation study showed that the failure of components can be detected in advance of the event. The advance notice period was found to range from 1 month to 2 years, as shown in Fig. 9.

4 Interpretation and prioritisation of results

The purpose of the SCADA-based condition monitoring process is to translate the trends and deviations produced from the models into actionable recommendations in order to assist in the improvement of turbine availability and reliability. This translation process incorporates a number of subjective elements. Deciding whether a trend is 'normal' or 'abnormal' involves consideration of a number of factors, including:

- The statistical accuracy of the model;
- The accuracy the model has in predicting historical failures at the site;
- Inaccuracy of predicting historical failures (the fraction of false positives produced by the model);
- The duration of the training period;
- The duration of the deviation produced by the model; and
- The magnitude of the deviation produced by the model.

To transform these potentially subjective considerations into a more predictable process, a scoring system should be implemented. An example of a suggested scoring system is shown in Table 3. The resulting score is known as the confidence factor (CF). The following categorisation is suggested:

CF, %	CF category
$0 < CF\% \leq 33$	low
$33 < CF\% \leq 67$	medium
$67 < CF\% \leq 100$	high

The resulting CF category can then be used to prioritise the actionable alerts that come from the condition monitoring process. This prioritisation process could help to ensure that the resources are expended on those alerts which are most likely to be associated with genuine failures. The proposed weightings and CF thresholds given above should be investigated further in order to optimise this prioritisation process as more experience is gained from applying the method.

5 Conclusions

SCADA-based condition monitoring can be used to monitor the condition of major components in the drivetrain. Three monitoring methods were applied to SCADA data from operational wind farms and the physical model approach was found to score highest when assessed on the range of relevant factors.

The physical model method was then assessed in greater detail in order to validate the results of the method against known failures at an operational wind farm. This validation study showed that it was possible to detect 24 out of 36 major component failures. The number of false positives was proportionally low at 3. An advance detection period of between 1 month and 2 years was achieved by the method. In a further development of the physical model, digital signals were incorporated and this enabled the detection of a generator failure.

A number of threshold exceedance alarms were produced by the method. To make best use of the results in a practical operational wind farm monitoring scenario, the results should be interpreted and prioritised before expending resources on further investigative actions. A method to enable prioritisation to be applied has been proposed. Suitable weightings and thresholds to apply during the prioritisation step will be refined as experience is gain in applying the method.

The signal trending and ANN techniques were not studied in detail. However, in future work, these two methods could be applied to the validation dataset in order to compare the outcome with the physical model.

When combined with a targeted inspection programme, the SCADA condition monitoring method described here has the potential to lead to a reduction of operational costs by making early intervention to repair or replace a component showing accelerated wear.

6 References

1 Tavner, P.J., Ran, L., Penman, J., Sedding, H.: 'Condition monitoring of rotating electrical machines' (Institution of Engineering and Technology, London, 2008), Series: IET Power and Energy

2 McMillan, D., Ault, G.W.: 'Quantification of condition monitoring benefit for offshore wind turibnes', *Wind Eng.*, 2007, **31**, pp. 267–285

3 Harman, K., Walker, R., Wilkinson, M.: 'Availability trends observed at operational wind farms'. Proc. 2008 European Wind Energy Conf. (EWEC 2008), Brussels, 2008

4 García Márquez, F.P., Tobias, A.M., Pérez, J.M.P., Papaelias, M.: 'Condition monitoring of wind turbines: techniques and methods', *Renew. Energy*, 2012, **46**, pp. 169–178

5 Boucher, B.: 'Lowering the cost of project using simple analysis of SCADA data – a real case example'. PHM Conf., New Orleans, 2013

6 Garcia, M.C., Sanz-Bobi, M.A., del Pico, J.: 'SIMAP: intelligent system for predictive maintenance application to the health condition monitoring of a windturbine gearbox', *Comput. Ind.*, 2006, **57**, pp. 552–568

7 Schlechtingen, M., Santos, I.F.: 'Comparative analysis of neural network and regression based condition monitoring approaches for wind turbine fault detection', *Mech. Syst. Signal Process.*, 2011, **25**, pp. 1849–1875

8 Kohonen, T.: 'Self-organising maps' (Springer, 2001, 3rd edn.)

9 Catmul, S.: 'Self-organising map based condition monitoring of wind turbines'. Proc. 2011 European Wind Energy Association Annual Event (EWEA 2011), Brussels, 2011

10 Gray, C.S., Watson, S.J.: 'Physics of Failure approach to wind turbine condition based maintenance', *Wind Energy*, 2010, **13**, (5), pp. 395–405

11 Feng, Y., Tavner, P.J., Crabtree, C.J., Feng, Y., Qui, Y.: 'Use of SCADA and CMS signals for failure detection and diagnosis of a wind turbine gearbox'. Proc. 2011 European Wind Energy Association Annual Event (EWEA 2011), Brussels, 2011

© The Institution of Engineering and Technology 2014

17521424, 2014, 4, Downloaded from https://ietresearch.onlinelibrary.wiley.com/doi/10.1049/iet-rpg.2013.0318 by CAPES, Wiley Online Library on [07/05/2024]. See the Terms and Conditions (https://onlinelibrary.wiley.com/terms-and-conditions) on Wiley Online Library for rules of use; OA articles are governed by the applicable Creative Commons License